Monolayer Formation

DOI: 10.1002/anie.200800737

Phosphine Oxide Monolayers on SiO_2 Surfaces**

*Roie Yerushalmi, Johnny C. Ho, Zhiyong Fan, and Ali Javey**

Molecular thin films utilizing phosphonates are widely used in a variety of chemical applications, such as surfactants, stabilization of nanoparticle suspensions, layer by layer film formation, and more.[1–4] Furthermore, surface chemistry is a valuable tool in the context of semiconducting materials.[5,6] To date, the studies of monolayer formation of phosphonates have mainly focused on phosphonic acids.[7–10] However, for certain applications, the less polar phosphine oxides are more desirable. Phosphine oxides are readily soluble in nonpolar organic solvents, such as toluene and mesitylene, and are compatible with many types of semiconducting materials. Importantly, these phosphorous derivatives do not have acidic functionality which can lead to uncontrolled etching or degradation of the substrate surfaces. Recently, we demonstrated a novel application using phosphine oxides for controlled nanoscale doping of materials by utilization of their surface chemical properties.[11] Herein, we report the details of monolayer formation of phosphine oxides on SiO_2 substrates, shedding light on the critical role of their chemical substituents in the assembly process. We find the monolayer formation process to be self-limiting, without applying specialized techniques as required for phosphonic acid thin films.[12,13] Furthermore, the precise nature of the binding interactions between the phosphine oxides and the SiO_2 substrate, and the uniformity and surface morphology of the self-assembled monolayers, are found to strongly depend on the chemical, electronic, and steric properties of the substituents.

The chemical binding interactions between the phosphine oxides and SiO_2 surfaces may involve packing interactions, hydrogen bonding, and/or covalent bonding, depending on the chemical substituents (Figure 1b). Such interactions can lead to monolayer formation involving the P=O molecular sites. Monolayer formation for precursors **1** and **2** was confirmed using X-ray photoelectron spectroscopy (XPS) and atomic force microscopy (AFM), whereas no surface reaction was observed for **3** (Figure 2). H-bonds and covalent bonds are expected to be energetically less favorable for **3** than for **1** and **2** because of the more electron-withdrawing substituents of the P=O group as compared to **1** and **2**. This

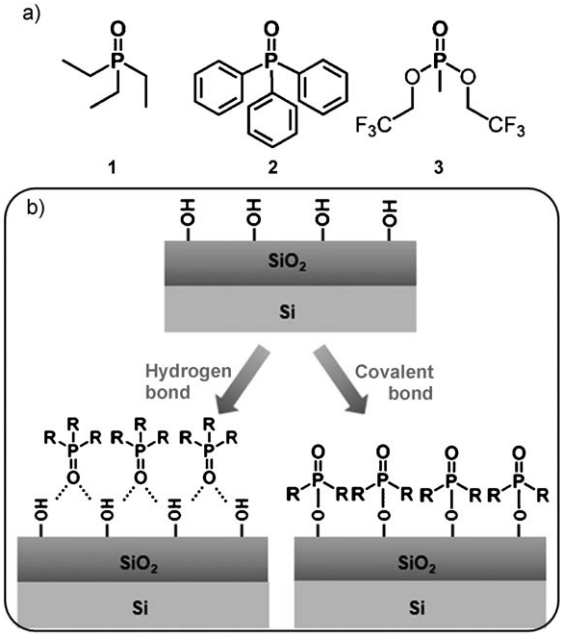

Figure 1. a) The molecular precursors used in this study, and b) proposed H-bond and covalent-bond monolayer formation on the SiO_2 surfaces.

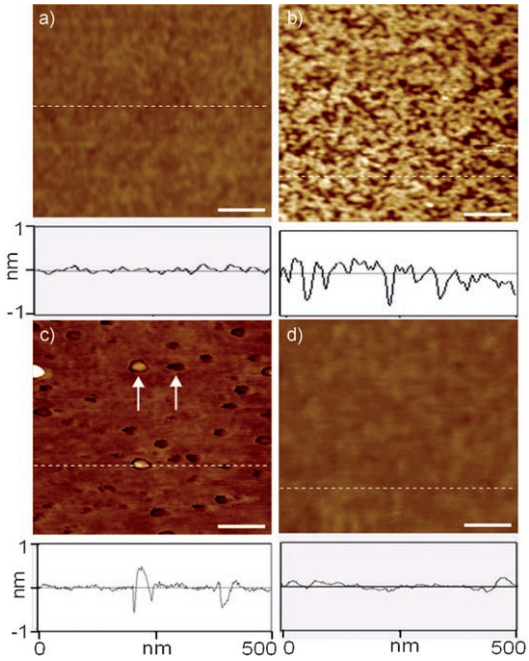

Figure 2. AFM topography images of SiO_2/Si substrates after reaction with a) only the solvent, and b)–d) solutions of **1**–**3**, respectively. Scale bars 100 nm, height range 2 nm. The arrows in (c) point to representative pin holes (black) and aggregates (white) in the monolayer with molecular dimensions (height and depth ca. 0.6 nm).

[*] Dr. R. Yerushalmi, J. C. Ho, Z. Fan, Prof. A. Javey
Department of Electrical Engineering and Computer Sciences
University of California at Berkeley, and Materials Science Division
Lawrence Berkeley National Laboratory
University of California at Berkeley (USA)
Berkeley, CA 94720
Fax: (+1) 510-643-7846
E-mail: ajavey@eecs.berkeley.edu

[**] This work was funded by a LDRD from Lawrence Berkeley National Laboratory, MARCO/MSD Focus Research Center, a Junior Faculty Award from UC Berkeley (A.J.), a Human Frontiers Science Program fellowship (R.Y.), and an Intel Foundation Ph.D. Fellowship (J.H.).

Table 1: Summary of the DFT calculated and experimental results for the reaction of **1**–**3** on SiO_2 surfaces.

	Calcd[a]		XPS $P2_p$	
	$-\Delta H_{Hb}$ [kcal mol^{-1}]	$-\Delta H_{cov}$ [kcal mol^{-1}]	Bulk [eV]	ML [eV]
1	7.6	12.7	133.2	135.2
2	3.9	14.4	133.4	134.0
3	−1.1	1.2	na	na

[a] Calculated hydrogen bond (Hb) and covalent (cov) bond values include zero point vibrational energy and basis set superposition error corrections at the B3LYP/6-311++G(d,p) level of theory.

result is in line with the computational analysis (Table 1), in which the calculated H-bond and covalent bond enthalpies for **3** are positive and slightly negative, respectively.

Figure 2 shows the AFM topography images of SiO_2 surfaces reacted with precursors **1**–**3**. Interestingly, **1** and **2** show markedly distinct structural and surface morphology characteristics, with high surface roughness (RMS roughness ca. 0.2 nm) for **1** and relatively smooth surface (RMS roughness ca. 0.1 nm) with low density of pin holes and defects for **2** (Figure 2b,c). From the AFM images, surface step amplitude of about 0.6 nm was observed for both **1** and **2**, which matches the expected height of the surface reacted molecules and suggests the monolayer formation on the SiO_2 surfaces with molecular-scale dimensions and features (Figure 3). Our computational analysis shows that the polar P=O group can form relatively strong and moderate bifurcated H-bond interactions with hydroxy groups of the SiO_2 layer (Table 1 and Figure 3). The distinct difference in the surface topography for the two types of monolayers may arise from the different molecular packing details of **1** and **2**. The phenyl groups of **2** can form π–π interactions between the molecules at the surface, whereas **1** lacks such interactions. Thus, the molecular orientation and packing of **1** is expected to be random owing to the absence of strong packing interactions between the short alkyl substituents, resulting in higher monolayer roughness. On the other hand, the π–π stacking interaction and noncovalent H-bond interactions with the SiO_2 surface allow for tight molecular packing, yielding highly uniform monolayer topography. For **3**, the surface topography was similar to a blank (only solvent) treated SiO_2 substrate, which along with the lack of XPS $P2_p$ signal suggest the lack of monolayer formation at the surface (Figure 2a,d), and in line with the computational analysis (Table 1).

To further study and characterize the bonding interactions, samples of **1** and **2** were washed with copious amounts of various solvents, including dichloromethane and methanol, before examination of the monolayers by AFM and XPS. Rinsing with dichloromethane had no observable effect on the quality of the monolayers, as confirmed by AFM and XPS, suggesting a significant bonding interaction between the molecules and the surface, and eliminating purely van der Waals interactions as being responsible. On the other hand, substrate washing with methanol resulted in an approximate threefold decrease in the $P2_p$ peak area for **1** and complete disappearance of the $P2_p$ peak for **2**. This result suggests a

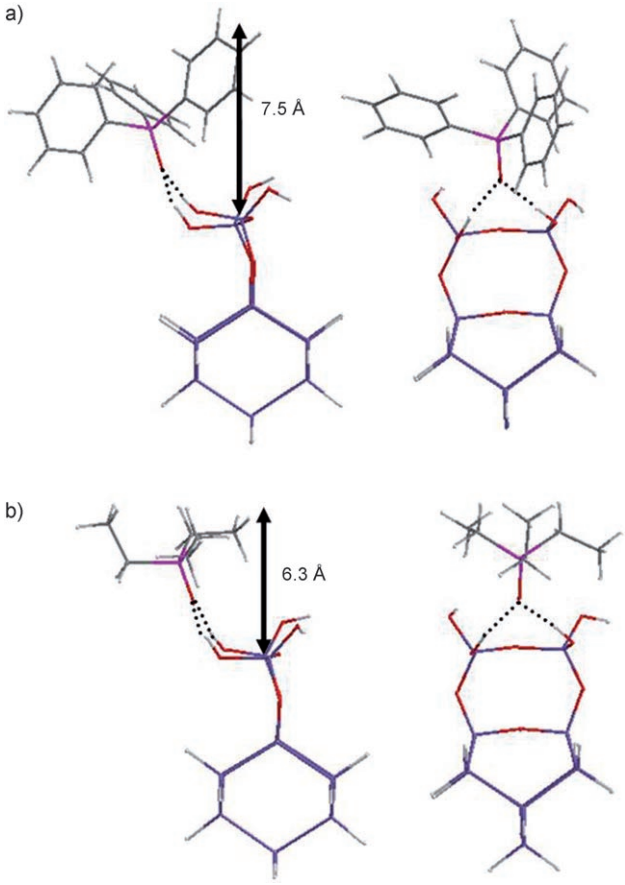

Figure 3. Calculated structures of triphenylphosphine (a) and triethylphosphine (b) H-bonded to the $Si_{11}O_8H_{16}$ cluster. The structures are shown in two perpendicular directions, and H-bond interactions are marked with broken lines. The black arrow indicates the maximal calculated height of 7.5 and 6.3 Å for **2** and **1**, respectively; all the structures are plotted at the same scale. H light gray, C dark gray, Si blue, P pink, O red.

partial monolayer removal of **1** and complete removal of **2** with a methanol rinse. As methanol forms strong H-bonds to the SiO_2 hydroxy groups as well as to the P=O groups, a vigorous methanol wash is expected to displace H-bonded molecules on the surface without affecting covalently attached molecules. Therefore, the methanol rinse results suggest that the primary surface bonding interaction for both **1** and **2** is H-bonding, with the interactions being stronger for **1**. Notably, the DFT computational results (Table 1) show that the covalent surface reaction is also energetically feasible for both **1** and **2**. However, these calculations do not take into consideration the reaction kinetics and the steric effects of the substituents at the surface. The bulky nature of the substituents, especially for **2**, is expected to limit the elimination reaction kinetics on the SiO_2 surface, and therefore reduce the rate of covalent bond formation. Our solvent washing experiments further support this hypothesis, although it is possible that for **1**, which contains the less bulky alkyl substituents, a small fraction of the molecules undergo elimination reactions at the surface and form covalent bonds to the SiO_2 surface, as the monolayer is only partially removed upon methanol exposure.

The surface bonding interactions were further examined by XPS analysis. The XPS results for **1** show a shift of $\Delta = (2 \pm 0.3)$ eV in the $P2_p$ binding energy for the reacted monolayer as compared to the bulk (Figure 4). For triphenylphosphine oxide **2**, a significantly smaller shift of $\Delta = (0.6 \pm 0.3)$ eV was observed for the $P2_p$ binding energy (Table 1), suggesting weaker surface chemical interactions for **2** compared to **1**. The triphenyl substituent is not only bulkier as compared to triethyl, but it is also less electron donating to the P=O group, making the electron density at the P=O group less polarized for **2** compared to **1**. This result is also supported by the significantly weaker calculated H-bond energy for **2** as compared to **1** (Table 1), and calculated dipole moments. The increase in $P2_p$ binding energies for the reacted monolayers of **1** and **2** compared to the bulk further supports the formation of significant binding interactions at the surface.

In summary, we have studied monolayer formation of phosphine oxides with different structural, chemical, and electronic properties on SiO_2 surfaces. We find that the bonding interactions and the monolayer defect density strongly depend on the precise nature of the substituents. Our results may have important implications for a number of applications utilizing phosphine oxide monolayers. In the future, further study of the surface reactivity and film formation kinetics of this class of molecules may provide valuable understanding of the underlying reaction mechanisms.

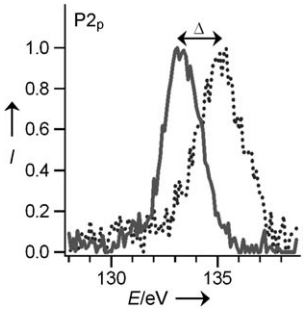

Figure 4. XPS spectra of the $P2_p$ core region, showing bulk trioctylphosphine oxide (solid line) and freshly prepared monolayer with solution of **1** (dashed line).

Experimental Section

Triethylphosphine oxide (**1**), triphenylphosphine oxide (**2**), and bis(2,2,2-trifluoroethyl) methylphosphonate (**3**) were used as the molecular precursors for surface interaction and monolayer formation studies on silicon dioxide surfaces. Si(100) substrates with native oxide or 50 nm of thermally grown oxide were cleaned by O_2 plasma treatment (30 W, 120 s), thoroughly washed with isopropanol and acetone, and dried with N_2. The cleaned samples were loaded into a dry N_2 glovebox and sealed in pressure tubes containing a 100 mM solution of the corresponding precursor (**1**–**3**) in mesitylene. The reactions were carried out at 120 °C for 2.5 h. Upon reaction completion, the solution was removed and the reacted substrates were washed with copious amounts of dichloromethane. Monolayer formation was investigated immediately by X-ray photoelectron spectroscopy (XPS), and atomic force microscopy (AFM). XPS data was collected with a PHI 5400 system with conventional non-monochromatic $Al_{K\alpha}$ radiation. Density functional theory (DFT) computational analysis was employed to study the molecular interactions on the SiO_2 surface. Geometry optimization and Hessian calculations were performed for molecules **1**–**3** in the gas phase. The interaction of molecules **1**–**3** with the Si–OH groups of the SiO_2 surface was modeled using the $Si_{11}O_8H_{16}$ cluster, as reported by Korkin et al.[14] The solvation energy was calculated by using the polarizable conductor computational model at a dielectric permittivity of $\varepsilon = 2.38$, as the value for toluene using fine grid integration.[15,16] We employed hybrid density functional theory techniques using Becke's three-parameter hybrid exchange functional with the widely used Lee–Yang–Parr gradient-corrected correlation functional.[17–19]

Received: February 14, 2008
Published online: May 6, 2008

Keywords: atomic force microscopy · hydrogen bonds · monolayers · phosphorus · surface chemistry

[1] S. Akhter, H. Lee, H. G. Hong, T. E. Mallouk, J. M. White, *J. Vac. Sci. Technol. A* **1989**, *7*, 1608.
[2] R. Frantz, J. O. Durand, M. Granier, G. F. Lanneau, *Tetrahedron Lett.* **2004**, *45*, 2935.
[3] P. H. Mutin, G. Guerrero, A. Vioux, *J. Mater. Chem.* **2005**, *15*, 3761.
[4] D. G. Byron, Q. Xu, J. C. Love, D. B. Wolfe, G. M. Whitesides, *Annu. Rev. Mater. Res.* **2004**, *34*, 339.
[5] W. J. Royea, A. Juang, N. S. Lewis, *Appl. Phys. Lett.* **2000**, *77*, 1988.
[6] S. Sun, G. J. Leggett, *Nano Lett.* **2007**, *7*, 3753.
[7] H. Y. Nie, M. J. Walzak, N. S. McIntyre, *J. Phys. Chem. B* **2006**, *110*, 21101.
[8] T. M. Putvinski, M. L. Schilling, H. E. Katz, *Langmuir* **1990**, *6*, 1567.
[9] E. L. Hanson, J. Schwartz, B. Nickel, N. Koch, M. F. Danisman, *J. Am. Chem. Soc.* **2003**, *125*, 16074.
[10] H. Lee, L. J. Kepley, H. G. Hong, S. Akhter, T. E. Mallouk, *J. Phys. Chem.* **1988**, *92*, 2597.
[11] J. C. Ho, R. Yerushalmi, Z. A. Jacobson, Z. Fan, R. L. Alley, A. Javey, *Nat. Mater.* **2008**, *7*, 62.
[12] I. Gouzman, M. Dubey, M. D. Carolus, J. Schwartz, S. L. Bernasek, *Surf. Sci.* **2006**, *600*, 773.
[13] B. R. A. Neves, M. E. Salmon, P. E. Russell, Jr., E. B. Troughton, *Langmuir* **2001**, *17*, 8193.
[14] A. Korkin, J. C. Greer, G. Bersuker V. V. Karasiev, R. J. Bartlett, *Phys. Rev. B* **2006**, *73*, 165312.
[15] K. Baldridge, A. Klamt, *J. Chem. Phys.* **1997**, *106*, 6622.
[16] A. Klamt, G. Schueuermann, *J. Chem. Soc. Perkin Trans. 2* **1993**, 799.
[17] C. Lee, W. Yang, R. G. Parr, *Phys. Rev. B* **1988**, *37*, 785.
[18] A. D. Becke, *J. Chem. Phys.* **1993**, *98*, 5648.
[19] Gaussian 03 (Revision C.02), M. J. Frisch, G. W. Trucks, H. B. Schlegel, G. E. Scuseria, M. A. Robb, J. R. Cheeseman, J. A. Montgomery, Jr., T. Vreven, K. N. Kudin, J. C. Burant, J. M. Millam, S. S. Iyengar, J. Tomasi, V. Barone, B. Mennucci, M. Cossi, G. Scalmani, N. Rega, G. A. Petersson, H. Nakatsuji, M. Hada, M. Ehara, K. Toyota, R. Fukuda, J. Hasegawa, M. Ishida, T. Nakajima, Y. Honda, O. Kitao, H. Nakai, M. Klene, X. Li, J. E. Knox, H. P. Hratchian, J. B. Cross, V. Bakken, C. Adamo, J. Jaramillo, R. Gomperts, R. E. Stratmann, O. Yazyev, A. J. Austin, R. Cammi, C. Pomelli, J. W. Ochterski, P. Y. Ayala, K. Morokuma, G. A. Voth, P. Salvador, J. J. Dannenberg, V. G. Zakrzewski, S. Dapprich, A. D. Daniels, M. C. Strain, O. Farkas, D. K. Malick, A. D. Rabuck, K. Raghavachari, J. B. Foresman, J. V. Ortiz, Q. Cui, A. G. Baboul, S. Clifford, J. Cioslowski, B. B. Stefanov, G. Liu, A. Liashenko, P. Piskorz, I. Komaromi, R. L. Martin, D. J. Fox, T. Keith, M. A. Al-Laham, C. Y. Peng, A. Nanayakkara, M. Challacombe, P. M. W. Gill, B. Johnson, W. Chen, M. W. Wong, C. Gonzalez, J. A. Pople, Gaussian, Inc., Wallingford CT, **2004**.

